Effects of Polydispersity on Relaxation Mechanisms and Viscoelastic Properties of Entangled Linear Polymers

Kwang-Sik Choi and In Jae Chung*

Department of Chemical Engineering, Korea Advanced Institute of Science and Technology, P.O. Box 131, Cheongryang, Seoul, Korea

Hee Young Kim

Chemical Engineering Laboratory 2, Korea Research Institute of Chemical Technology, P.O. Box 9, Daedeogdanji, Korea. *Received November 30, 1987; Revised Manuscript Received March 8, 1988*

ABSTRACT: A blending law for the relaxation spectrum is proposed in order to describe the enlargement of effective entanglement spacing due to constraint release. In binary blend the short chain (denoted as 1-chain) relaxes mainly by reptation with the characteristic relaxation time T_{d1}, whereas the long chain (denoted as 2-chain) shows three stage relaxation behaviors, i.e., reptation in the original tube of the diameter a for time $t < T_{d1}$, local equilibration of the chain conformation for $T_{d1} < t < T_{21}$ (T_{21} means the tube renewal time), and thereafter reptation again in a tube expanded to the diameter $a_2' = a\phi_2^{-\nu/2}$ with terminal relaxation time $T_{d2} = \phi_2^{\nu} T_{d2}°$, where the index ν varies with the blend ratio R (=M_2/M_1) from 0 when $R = 1$ to α (=1–1.25) when $R \to \infty$, ϕ_2 represents the volume fraction of 2-chains, and $T_{d2}°$ means the relaxation time for pure state of 2-chains. To discuss these relaxation mechanisms, the calculated dynamic moduli are compared with experimental data. The characteristic relaxation times obtained from the experimental dynamic moduli show T_{21} and T_{d2} decrease and increase with increasing ϕ_2, respectively, as predicted from our molecular picture. So as to test the compositional dependence, terminal viscoelastic properties such as zero-shear viscosity (η_0) and recoverable compliance ($J_e°$) are compared with many literature data. The present law describes well rheological properties over wide ranges of ϕ_2 and R. Especially, at high concentration it predicts $\eta_0 = \phi_2^{1+2\nu}(\eta_0)_2$ and $J_e° = \phi_2^{-(1+\nu)}(J_e°)_2$ over all the ranges of R. The onset of entanglement between different longer chains is well predicted by their component molecular weight ratio as $\phi_c = (M_1/M_2)^{1/\nu}$.

Introduction

The properties of polymers depend on their large-scale molecular structures, i.e., molecular weight (MW), molecular weight distribution (MWD), and long-chain branching.[1,2] While the branch effects on the rheological behavior are still being studied,[2-5] experimental studies of the entangled linear polymers with narrow MWD have been done over the last 30 years.[1,2] And for the effects of polydispersity for entangled linear chains, binary blends of nearly monodisperse fractions have been investigated extensively.[6-12]

The zero-shear viscosity η_0 depends on their weight-average molecular weight (M_w) as the power law $\eta_0 \propto M_w^{3.4}$.

The recoverable compliance $J_e°$ is very sensitive to MWD. Its value increases rapidly as the volume fraction ϕ_2 of longer chains (designated as 2-chains with MW of M_2) increases in a shorter chain (designated as 1-chain with MW of M_1) matrix, and after the maximum compliance $(J_e°)_{max}$ is reached, with increasing ϕ_2 it approaches $(J_e°)_2$ along the power law, $(J_e°)_B = (J_e°)_2/\phi_2^{\beta}$ ($1 < \beta <$ 2–2.4). As the binary blend ratio, $R = M_2/M_1$, increases, the $(J_e°)_{max}$ and the $(\phi_2)_{max}$ at this value increase and decrease, respectively.

According to the tube model, the constraint release mechanism describes well the MWD effects on rheological properties.[10-12] The criterion for the significance of tube renewal effects was proposed by Daoud and de Gennes.[13] If the pure tube renewal time of a 2-chain isolated in 1-chains, $T_{r2}°$, is larger than the time for a 2-chain to disengage a tube by only reptation and contour length fluctuation, $T_{d2}°$, the relaxation process is dominated by reptation and nearly independent of ϕ_2 (case I). Otherwise, i.e., if $T_{d2}° > T_{r2}°$, constraint release effects become very important (case II). In this case, after tube-forming 1-chains released the tube, the conformation of 2-chain reaches a reequilibrium state with expanded tube diameter, and thereafter the 2-chain disengages the enlarged tube with the characteristic relaxation time T_{d2} dependent on ϕ_2. Recent measurement by Struglinski and Graessley[12] on rheological properties for various binary mixtures of polybutadiene (PB) cover the former case. Several polystyrene (PS) mixtures[6-11] investigated to date belong mostly to the latter case.

Here we consider case II by observing the individual contribution of each component to stress relaxation behavior. It can be observed rather directly in the dynamic experiments, for example, a Cole–Cole plot (G'/ω versus G''/ω)[9] or dynamic moduli (G' or G'' versus ω),[12] where G' and G'' are respectively the storage and loss moduli and ω is the frequency. In the high frequency region, all chains participate in the entanglement network, giving a rubberlike response in that scale of frequencies. In other words, up to a relaxation time T_{d1} of the short chain the tube conformation is fixed. At an intermediate frequency, an inflection frequency ω_p in the storage modulus curve G' defines a secondary plateau modulus of the blend, $(G')_p$, which is associated with the low-frequency relaxation domain. That is, the tube renewal by the short chains is completed in the corresponding time scale. Finally, in the low-frequency region, only the long chain exhibits viscoelastic properties and the short chain shows solventlike molecules. The T_{d2} decreases with decreasing ϕ_2.

Various blending laws have been proposed in order to describe the polydispersity effect mainly in binary blends. They mostly use simple combinations of the component spectra of relaxation time to force agreement with such features as $\eta_0 \propto M_w^{3.4}$ and the constancy of the plateau modulus $G_N°$.[10,11,14,16]

Kurata[16] proposed a blending law on the basis of the tube model of Doi and Edwards,[17] but he did not consider constraint release due to tube renewal. Recently, Watanabe et al.[11] proposed an experimental blending law including another relaxation mechanism by tube renewal. Some determinations of characteristic times from relaxation spectra $H(\tau)$ are somewhat ambiguous. More recently,

* To whom all correspondence should be addressed.

0024-9297/88/2221-3171$01.50/0

Montfort et al.[10] proposed an expression for the tube renewal time of a long chain in a binary blend based on Graessley's treatment which has assumed the reptation of a chain and its tube-renewal motion are independent each other. But the relaxation processes are not clearly independent but rather sequential. That is, after shorter chains relax the terminal relaxation of longer chains should be affected by tube renewal.

Kim and Chung[18] have proposed a modified tube model, they called the equivalent primitive chain model, with consideration of the significance of constraint release by local tube renewal in accounting for the relaxation process of a long chain in the binary blend. In their theory the longest relaxation time of a model chain is related to the component relaxation times in the pure state, $T_{d2}°$, and ϕ_2. Tube renewal time T_{21} must be decreased as ϕ_2 increases because 2–2 entanglements act as cross-link points even though 1-chains were released. Thus the tube reorganization might occur only between 2–2 entanglement points.

In this paper, we discuss the effects of ϕ_2 on tube renewal and terminal relaxation of large linear chains for the system of case II. On the basis of the modified tube model and experimental results from this work and literature data, we give a blending law to describe the effects of ϕ_2 on relaxation of 1-chains, tube renewal, and relaxation of 2-chains.

Tube Model and a Blending Law

1. Monodisperse Polymers. Doi and Edwards extended the de Gennes' reptation concept[19] to explain rheological properties of entangled polymeric liquids. If the reptation, i.e., the diffusion of a model chain in a fixed obstacles, is the dominant mechanism for the chain motion even in the absence of the permanent network matrix, the longest relaxation time T_{rep} is given by

$$T_{rep} = K\frac{M^3}{M_e} \tag{1}$$

where K is the temperature dependent constant which is related to the friction coefficient associated with each statistical segment (Kuhn's segment), M denotes MW of a fraction, and M_e means the MW between two slip-links.

Doi[20] has recently proposed that the discrepancy between $\eta_0 \propto M^3$ by pure reptation and widely observed $\eta_0 \propto M^{3.4}$ is mainly caused by thermal fluctuations of the primitive path length. By assuming that the contour-length distribution function is Gaussian around equilibrium contour length L_{eq}, he showed that the time-average of the fluctuation magnitude δL is given by

$$\delta L/L_{eq} = (M_e/M)^{1/2} = N^{-1/2} \tag{2}$$

The longest relaxation time $T_d°$ for chains with N primitive path steps is related to that for pure reptation T_{rep}:

$$T_d° = T_{rep}(1 - \epsilon N^{-1/2})^2 \tag{3}$$

where the constant ϵ is taken to be unity in his smoothed version, and his more completed derivation yields $\epsilon = 1.47$. The above expression is in good agreement with experimental observation $T_d° \propto M^{3.4}$ for $2 < N < 100$.

More recently, Lin[21] also discussed the fluctuation effect on a reptating chain in his general linear viscoelastic theory. He dealt with reptation and fluctuation as two decoupled processes. The treatments by Doi and Lin yield a quantitatively similar MW dependence of viscoelastic constants.

2. Binary Mixtures. A binary blend composed of two components, short chains and long chains with volume (or weight) fractions ϕ_1 and ϕ_2, respectively, and with $M_1, M_2 \gg M_e$, of the same linear flexible polymer is the most critical case for accounting the polydispersity effects. In the blend, another relaxation mode becomes significant in addition to reptation and contour length fluctuation. This process is the effect of the motion in the surrounding short chains on the relaxation of long chains.

Klein[22] has treated the constraint release process by considering the tube as a virtual Rouse chain consisting of N_2 ($=M_2/M_e$) submolecules. He estimated the characteristic time for the complete renewal of the tube conformation as

$$T_{r2}° = kT_{d1}N_2^2 \tag{4}$$

where k is a proportionality constant ($\simeq 1/3\pi^2$) and T_{d1} a characteristic time associated with the release of tube constraints.

Graessley[23] also developed a model including constraint release contributions based on the bond-flip model of Orwoll and Stockmayer by assuming that two mechanisms, relaxation of a model chain and constraint release, are uncorrelated with each other. Up to date, blends studied from the standpoint of molecular picture are mostly based on his model.

Here we consider a modified tube model by Kim and Chung,[18] who have proposed it with the consideration of the significance of constraint release by local tube renewal. In a binary mixture, a 2-chain shows different relaxation behavior from an 1-chain which relaxes only by reptation and contour length fluctuation. Up to a time order T_{d1} the tube conformation confining the 2-chain is fixed, i.e., the 2-chain relaxes only by reptation in the tube with the effective entanglement spacing M_e for $t < T_{d1}$.

For time larger than T_{d1} the 2-chain renews its conformation not only by its own reptation but also by the local constraint release. If T_{21} is the time when the constraint release is completed, $T_{21} - T_{d1}$ might be equivalent to the longest Rouse relaxation time of local segment between two entanglement points formed by 2–2 couplings:

$$T_{21} - T_{d1} = kN_t^2T_{d1} \tag{5}$$

where N_t is the number of primitive path steps between two slip-links within a 2-chain. This number is inversely proportional to ϕ_2 and written as

$$N_t = N_2/[(N_2 - 1)\phi_2 + 1] \tag{6}$$

The schematic representation of the relaxation mechanism of a 2-chain is shown in Figure 1. According to eq 5, the tube renewal time decreases with increasing ϕ_2. This physical basis makes a difference in earlier theories treated by Klein and Kraessley and in many experimental analyses[10,11] based on their model.

For $t > T_{21}$ only the high MW 2-chains exhibit viscoelastic properties, and the low MW 1-chains act as a viscous liquid. Thus when the tube renewal is completed the effective entanglement spacing M_{e2}' is related to the actual spacing M_e and the composition ϕ_2 by

$$M_{e2}'/M_e = \phi_2^{-\nu} \tag{7}$$

where ν means the degree of departure from solventlike dependence and changes from α (=1–1.25) at $N_1/N_2 \to 0$ to zero at $N_1/N_2 \to 1$. Thus the ν can be approximated as

$$\nu = \alpha(1 - N_1/N_2) \tag{8}$$

where α varies slightly with the polymer species.[10] Recent

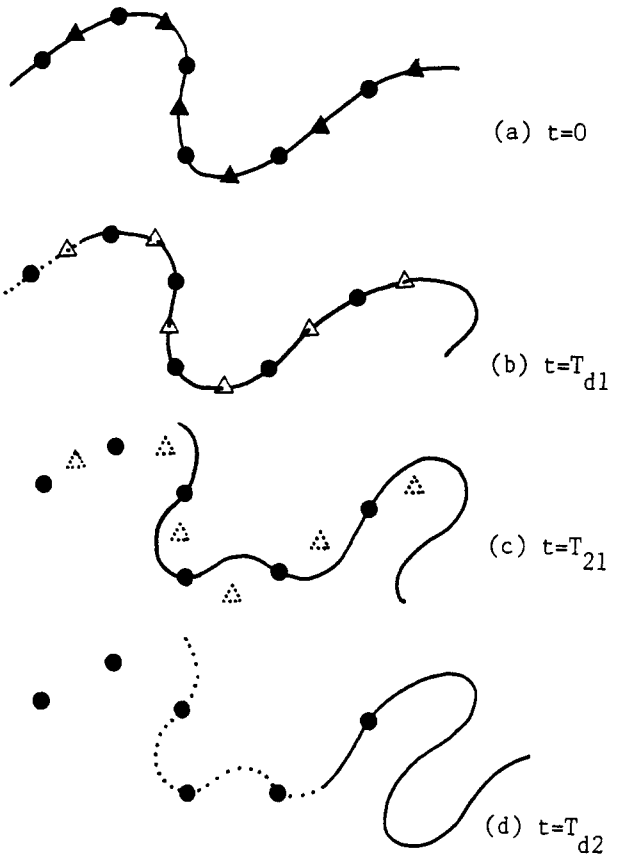

Figure 1. Schematic illustration of the relaxation mechanism of the long chain in the binary blend: (a) original chain conformation (denoted by thick line) in surrounding short (▲) and long (●) chains; (b) constraint release begins by the evaporation of the short chains; (c) a new conformation is generated by local tube renewal; (d) the long chain disengages by reptation alone after reequilibration of chain conformation.

experiments on polystyrene have indicated that $\alpha = 1.0$.[24] As the original square end-to-end distance of the primitive step a^2 is proportional to M_e, the diameter of the enlarged tube a_2' at $t > T_{21}$ is proportional to M_{e2}', i.e., $a_2' = a\phi_2^{-\nu/2}$. The 2-chain disengages the tube expanded by only reptation.

The effective entanglement spacing has a deep relation with viscoelastic properties. For example, the plateau modulus is inversely proportional to the entanglement spacing and can be represented by summing up the respective contributions of each component for a blend:

$$(G_N^\circ)_B = \phi_1\frac{\rho RT}{M_e} + \phi_2\frac{\rho RT}{M_e} = G_N^\circ \qquad \text{for} \quad t < T_{c1} \tag{9}$$

where $(G_N^\circ)_B$ means the plateau modulus for the blend and is equal to the so-called plateau modulus G_N° in this time region, ρ is the density of the blend, R is the universal gas constant, and T is the temperature. From $t = T_{21}$ when the 1-chains act as a solvent, the modulus shows a second plateau $(G_N^\circ)_B'$ attributed to only 2-chains in the blend:

$$(G_N^\circ)_B' = \phi_2\frac{\rho RT}{M_{e2}'} = G_N^\circ\phi_2^{1+\nu} \qquad \text{for} \quad t \geq T_{21} \tag{10}$$

Finally, for time larger than T_{21} the relaxation of the 2-chain is equivalent to the reptational disengagement of an original 2-chain with entanglement spacing M_{e2}'. Thus the longest relaxation time T_{d2} is

$$T_{d2} = \phi_2^{\nu}T_{d2}^\circ \tag{11}$$

According to eq 5 and 11 the 2-chain always finishes its terminal relaxation after the completion of the local tube renewal process.

In the blends of $\phi_2 < \phi_c$ where the interactions among different 2-chains are not effective, the dynamics of the 2-chain will show rather complex behavior. That is, in the infinite dilute region where the 2-chain is isolated in 1-chains and 2–2 interaction is negligible, the 2-chain renews its conformation only by tube renewal after the relaxation of 1-chains. But in semidilute region where 2–2 interactions are important even though the entanglement between 2-chains does not exist, the tube renewal by the 1-chains constraining the 2-chain is no more free due to the restricted Rouse-like tube renewal. Here we neglect these behaviors in the low-concentration blends with $\phi_2 < \phi_c$ and regard in the same light the behavior at ϕ_c which scaled as follows.[18] As the volume fraction of the 2-chain decreases in the 1-chain matrix, M_{e2}' has the value of its upper bound $(M_{e2}')_{max}$ scaled as M_eN_2/N_1, and thus the critical composition ϕ_c corresponding to the onset of entanglement between 2-chains is

$$\phi_c = [N_1/N_2]^{1/\nu} \tag{12}$$

From this and eq 8 it is shown that the ϕ_c decreases from $e^{-1/\alpha}$ to N_1/N_2 as the blend ratio R increases from 1 to infinitity, respectively.

3. Blending Law. After sudden step strain, every molecule contributes independently to stress relaxation and thus the relaxation spectrum $H_B(\tau)$ of a mixture can be expressed as[17]

$$H_B(\tau) = \sum_i \phi_i H_i(\tau) \tag{13}$$

where $H_i(\tau)$ means the relaxation spectrum for the i-component.

Experimentally, the average relaxation time of the short chain increases from its pure component value to a somewhat larger value with increasing ϕ_2.[11,12] In our molecular picture on the relaxation mechanisms in binary blends, however, the relaxation mode of the short chain is identical with that of the bulk. This is reasonable because the reptation and the contour length fluctuation are dominant even though the 2-chains constrain the 1-chain. Then, it is possible to assume that $H_1(\tau)$ in the binary blend is the same as $H_1^\circ(\tau)$ for the purely monodispersed state of 1-chains:

$$H_1(\tau) = H_1^\circ(\tau) \tag{14}$$

which is described schematically in Figure 2a.

The relaxation behavior of the 2-chain is somewhat different from that in the bulk as noted above. Up to the time of order T_{d1}, The constraints on the 2-chain due to the 1-chains are effective and the blend behaves as an entanglement network. On the other hand, on the time scale $\tau > T_{d1}$, the constraints on the 2-chain are released by the reptational motion of 1-chains. When the constraint release is completed, the tube confining the 2-chain partly generates a new one. The characteristic time T_{21} corresponding to this local tube renewal process is given by eq 5. The relaxation spectrum during the tube renewal probably is a Rouse-wedge type. After tube reorganization, i.e., for $\tau > T_{21}$, the 2-chain relaxes again by reptation in the tube with entanglement spacing M_{e2}' $(=\phi_2^{-\nu}M_e)$ and the short chain behaves as a somewhat solvent-like chain. In Figure 2b is shown the relaxation mode of the 2-component, which is represented as a sum of respective contributions by 2–1 and 2–2 interactions. In this figure, H_{21} represents the contribution by 2–1 interactions to the spectrum of the 2-component including reptation and tube renewal and H_{22} describes the spectrum related to only the

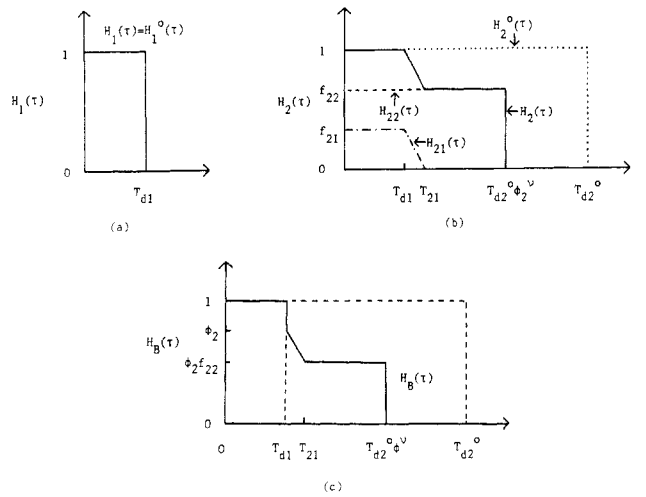

Figure 2. Schematic diagram representing the reduced relaxation modes and spectrum of each component and a blend. (a) The relaxation mode of 1-component; the 1-chain relaxes by reptation. (b) The relaxation mode of 2-component; the 2-chain relaxes by reptation in an original tube for $\tau < T_{d1}$, by tube renewal for $T_{d1} < \tau < T_{21}$, and by reptation in an expanded tube for $\tau > T_{21}$. (c) The relaxation spectrum of a blend of ϕ_2; the dashed lines represent the spectra at two extreme condition, $\phi_2 = 0$ and 1.

disengagement of the 2-component with T_{d2} in the tube consisting only of 2–2 entanglements.

Since $H_2(\tau)$ is affected by the release of 2–1 and 2–2 entanglements and by entanglement density, the following equation can be chosen reasonably:

$$H_2(\tau) = H_{21}(\tau) + H_{22}(\tau) = f_{21}H_2^\circ(\tau/\lambda_{21}) \times [U(\tau) + \{P_{21}(\tau) - 1\}U(\tau - T_{d1})] + f_{22}H_2^\circ(\tau/\lambda_{22}) \quad (15)$$

where λ_{21}, λ_{22} refer to the shifting factors for the relaxation times and f_{21}, f_{22} are weighting factors corresponding to spectrum intensity due to the composition ϕ_2. $U(\tau)$ is a unit step function and $P_{21}(\tau)$ represents an intensity factor for the local tube renewal process as a function of time, which is obtainable from the variation of the transient effective entanglement spacing $M_{e2}(\tau)$ increasing from M_e at $\tau = T_{d1}$ to M_{e2}' at $\tau = T_{21}$.

From eq 5 and 11, the following equations hold for λ_{21} and λ_{22}:

$$\lambda_{21} = T_{21}/T_{d2}^\circ \simeq (1 + kN_t^2)(M_1/M_2)^{3.4} \quad (16)$$

$$\lambda_{22} = T_{d2}/T_{d2}^\circ = \phi^\nu \quad (17)$$

where ϕ is equal to ϕ_2 if the 2-chains are concentrated in the blend; otherwise all the parameters such as N_t, T_{d2}, and M_{e2}' are equal to their respective values at ϕ_c. On the other hand, the intensity factors, f_{21} and f_{22}, are obtained from the effective entanglement spacing as a function of ϕ_2:

$$f_{22} = M_e/M_{e2}' = \phi^\nu \quad (18)$$

$$f_{21} = 1 - f_{22} = 1 - \phi^\nu \quad (19)$$

The relaxation spectrum of the 2-component in eq 15 can be divided into three regions, i.e., a box type at $\tau < T_{d1}$, a wedgelike spectrum at $T_{d1} < \tau < T_{21}$, and a box type at $\tau > T_{21}$ as shown in Figure 2b:

$$\begin{aligned} H_2(\tau) &= H_2^\circ(\tau) \quad \text{at} \quad \tau < T_{d1} \\ &= (f_{21}P_{21} + f_{22})H_2^\circ(\tau) \quad \text{at} \quad T_{d1} < \tau < T_{21} \\ &= f_{22}H_2^\circ(\tau/\lambda_{22}) \quad \text{at} \quad \tau > T_{21} \end{aligned} \quad (20)$$

In the transient region of $T_{d1} < \tau < T_{21}$, it is expected that the 2-component shows the wedge-type spectrum with its intensity proportional to $M_e/M_{e2}(\tau)$. Unfortunately the variation of $M_{e2}(\tau)$ with time cannot be described explicitly. If we approximate the $M_{e2}(\tau)$ as a linear function satisfying two limiting conditions, $M_{e2}(T_{d1}) = M_e$ and $M_{e2}(T_{21}) = M_{e2}'$, the P_{21} can be obtained as

$$P_{21}(\tau) = \frac{T_{21} - \tau}{(T_{21} - \tau) + \phi_2^{-\nu}(\tau - T_{d1})} \quad (21)$$

which approaches unity at $\tau = T_{d1}$ and zero at $\tau = T_{21}$. According to this equation, the second line in the eq 20 means that the intensity of the wedgelike spectrum is proportional to $1/\tau$, which is slightly different from a Rouse-like wedge-type spectrum[1] with the intensity proportional to $\tau^{-1/2}$.

The relaxation spectrum of a blend of ϕ_2 is shown in Figure 2c where the dashed lines represent the spectrum at two limiting conditions, $\phi_2 = 0$ and 1. In the region $\tau < T_{d1}$, the relaxation spectrum of the blend is simply written as the weight average of that of each pure component because of the fixed tube in the time scale considered like eq 9. In the region $\tau \geq T_{d1}$, when the contribution of 1-component is null, only the 2-component contributes to the spectrum by its concentration showing wedge- and box-type spectrum.

Although the wedgelike spectrum exists in the tube renewal region, the contribution of this spectrum probably does not differ much from that of the box-type spectrum if the tube renewal time is very short relative to the terminal relaxation time after constraints are released. Thus the relaxation spectrum $H_B(\tau)$ for the mixture of ϕ_2 can be written as

$$H_B(\tau) = \phi_1 H_1^\circ(\tau) + \phi_2(1 - \phi^\nu)H_2^\circ(\tau/\lambda_{21}) + \phi_2\phi^\nu H_2^\circ(\tau/\lambda_{22}) \quad (22)$$

from eq 13, 14, and 20 and by putting $P_{21} = 1$, where ϕ is equal to ϕ_2 when $\phi_2 > \phi_c$, otherwise $\phi = \phi_c$. If we know only the spectra of each pure component, the equation above can be applied over all the ranges of composition ($0 \leq \phi_2 \leq 1$) in the blend and can predict general linear viscoelastic properties.

Table I
Molecular and Rheological Characteristics of Polystyrene at 160 °C

sample	M_n	M_w	M_w/M_n	η_0, P	J_e°, cm²/dyn
M95	93 300	96 700	1.036	5.04×10^5	9.76×10^{-7}
M575	485 000	528 000	1.078	2.60×10^8	1.46×10^{-6}
B95/575-0.2	111 300	183 400	1.648	5.66×10^6	2.60×10^{-5}
B95/575-0.4	137 900	270 200	1.960	2.02×10^7	6.98×10^{-6}
B95/575-0.6	181 100	357 000	1.971	4.60×10^7	4.79×10^{-6}

Experimental Section

The nearly monodisperse fractions used in this study are standard polystyrenes which were manufactured by Pressure Chemical Co. The samples, fractions and binary blends, were prepared by dissolving weighed amounts of the individual components in a large excess of benzene at a concentration of about 0.02 g/cm³. Then the solvent was removed by freeze-drying under vacuum of about 0.1–0.2 mmHg at room temperature. The samples were further dried at 60 °C for 2 days in a vacuum oven so as to remove any possible traces of the benzene. The dried samples were vacuum-molded at about 160–170 °C to a diameter of 25 mm and a thickness of 2 mm. The molecular and rheological characteristics of samples are summarized in Table I. Figure 3 shows the MWD curves of binary blends of B95/575.

The dynamic shear measurements were performed with a parallel-plate rheometer (RDS-7700) at several temperatures between 140 and 230 °C. Master curves of the dynamic moduli were obtained at a reference temperature T_R = 160 °C.

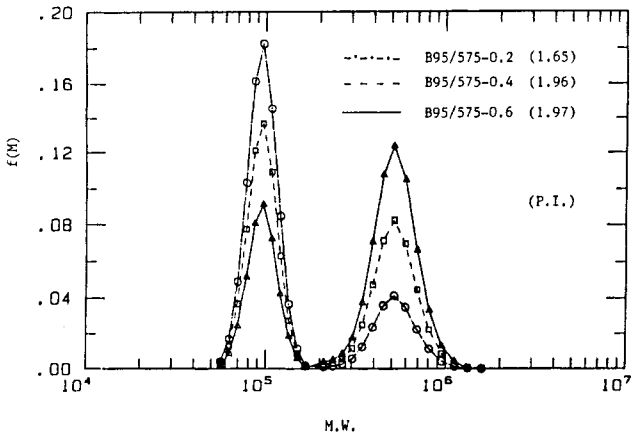

Figure 3. Molecular weight distribution of binary blends of M95 and M575. Symbols denote the specific components of the blends.

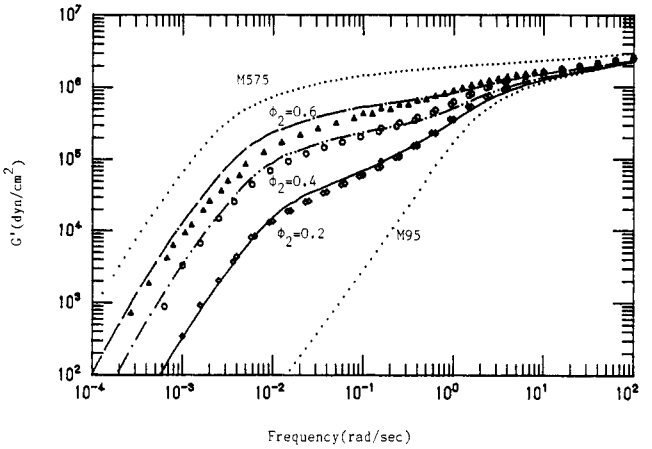

Figure 4. Storage moduli G' for B95/575 blends. Symbols denote superposed data reduced at 160 °C. Dotted lines denote data for monodisperse fractions. Other curves represent calculated values by the present law.

Discussion

1. Dynamic Moduli. The storage and loss moduli are related to the relaxation spectrum as[1]

$$G'(\omega) = \int_{-\infty}^{\infty} \frac{\omega^2\tau^2}{1+\omega^2\tau^2} H(\tau)\, \mathrm{d}\ln\tau \qquad (23)$$

$$G''(\omega) = \int_{-\infty}^{\infty} \frac{\omega\tau}{1+\omega^2\tau^2} H(\tau)\, \mathrm{d}\ln\tau \qquad (24)$$

Applying eq 22, G'_B and G''_B in the blends can be obtained:

$$G'_B(\omega) = \phi_1 G_1'(\omega) + \phi_2(1-\phi^\nu) G_2'(\omega\lambda_{21}) + \phi_2\phi^\nu G_2'(\omega\lambda_{22}) \qquad (25)$$

$$G_B''(\omega) = \phi_1 G_1''(\omega) + \phi_2(1-\phi^\nu) G_2''(\omega\lambda_{21}) + \phi_2\phi^\nu G_2''(\omega\lambda_{22}) \qquad (26)$$

Figures 4 and 5 show the master curves, G' and G'', by time–temperature superposition (denoted by symbols) and the curves estimated from the blending law (denoted by solid lines) for B95/575 blends, respectively. The dotted lines in these figures represent G' and G'' for each pure state, M95 or M575. On the assumption that the complex moduli for pure bulk states are nondiscriminatory from purely monodispersed states, we calculate the rheological properties of the blends. The molecular weights of both chains are larger than the molecular weight between two entanglement points, M_e (=18 000 for PS). As shown in these figures, it seems to be reasonable that the wedge-type

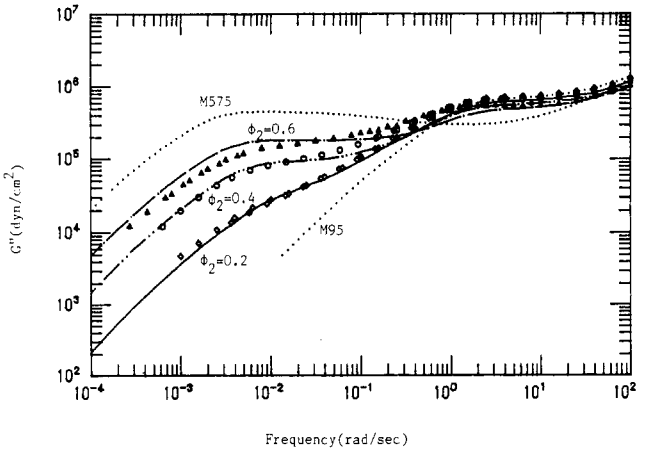

Figure 5. Loss moduli G'' for B95/575 blends. Symbols and curves are identified in Figure 4.

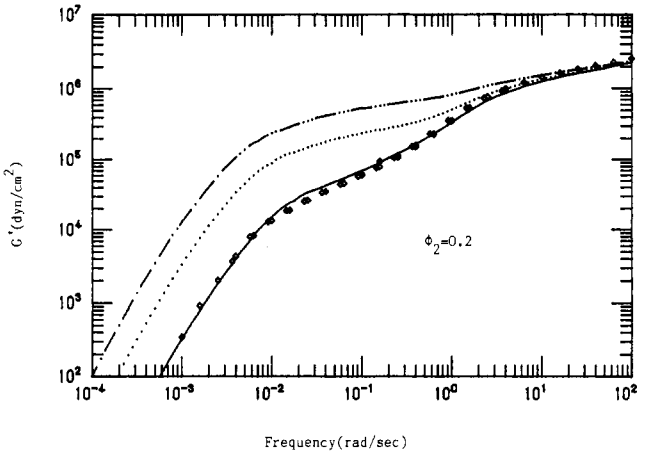

Figure 6. Storage modulus G'' for B95/575-0.2 blend at 160 °C: (—) present law; (···) Kurata;[16] (-···-) Doi and Edwards.[17]

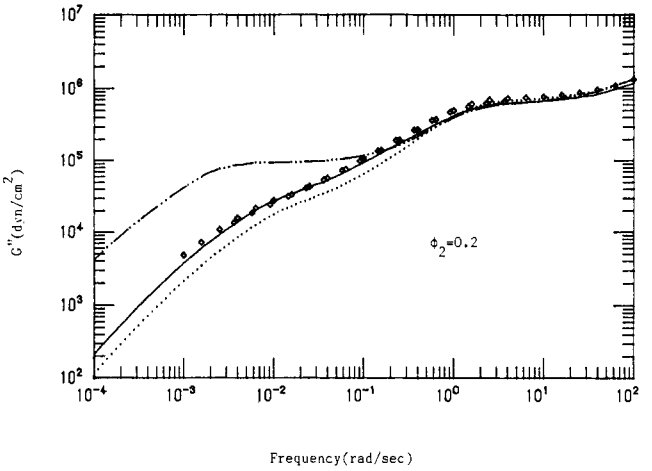

Figure 7. Loss modulus G'' for B95/575-0.2 blend at 160 °C. The curves are identified in Figure 6.

spectrum is replaced by a box-type one since the time T_{d2} is much greater than T_{21}. As the blend ratio increases, however, the overestimation is expected, due to the approximation of the wedge type to the box type in transient region.

The master curves have a shoulder, the height of which increases with increasing ϕ_2, and the two-step rubbery plateau is well predicted by the present blending law. The details of G' and G'' master curves will be discussed later.

In Figures 6 and 7 the present blending law is compared with other blending laws for the mixture of $\phi_2 = 0.2$. The

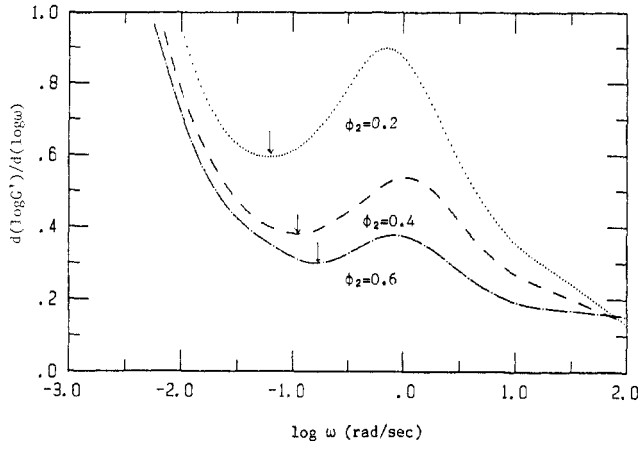

Figure 8. Variations of d(log G')/d(log ω) with frequency. The inflection frequencies in G' versus ω are determined by the arrows.

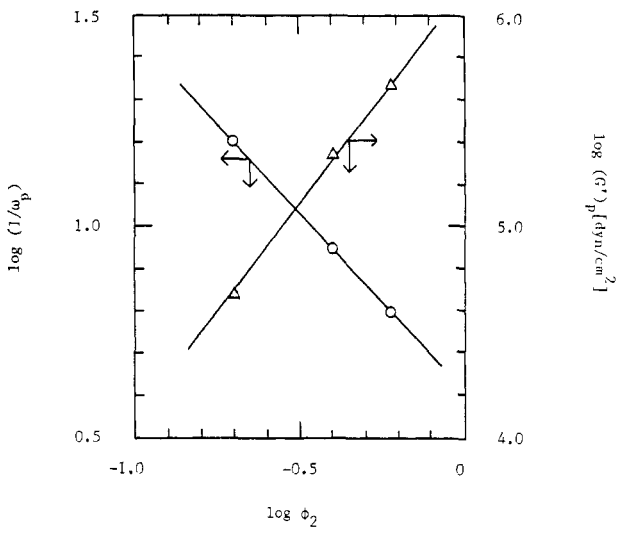

Figure 9. Concentration dependences of the inverse of inflection frequencies, $1/\omega_p$ (○), and the corresponding intermediate storage modulus $(G')_p$ (△).

dashed line represents the simple weight additivity rule[17] with no shift and weighting factor, which leads to

$$H_B(\tau) = \phi_1 H_1^\circ(\tau) + \phi_2 H_2^\circ(\tau) \quad (27)$$

The equation above will be applicable if the ratio of respective component molecular weights is very low ($R \to 1$). The dotted line denotes the blending law proposed by Kurata[16] who determined that only the terminal relaxation time of the 2-chains is shifted toward lower relaxation time:

$$H_B(\tau) = (1 - \phi_2^2)H_1^\circ(\tau) + \phi_2^2 H_2^\circ(\tau/\phi_2) \quad (28)$$

which is applicable only in the blends of high R and ϕ_2. Since he did not consider the local tube renewal mechanism and the dependence of terminal relaxation time on R, his model is not accountable for the behavior at the intermediate and lower frequency region. The solid line represents the plot of eq 25 and 26. The blending law proposed here is well fitted with experimental data not only in the region of high and low frequency domains but also in the intermediate region. The local tube renewal effect becomes more important at low ϕ_2 as noted in eq 5. Our blending law, eq 22, approaches eq 27 at $R \to 1$ or high ϕ_2 and eq 28 at $R \to \infty$ and high ϕ_2. That is, eq 27 and 28 satisfy our blending law at somewhat extreme conditions of R and ϕ_2.

2. Characteristic Relaxation Times. As shown in Figures 4 and 5, eq 25 and 26 give slightly underestimated values in the high-frequency region. And by careful examination of the upper plateaus for G' and G'', it can be noticed that the plateau shifts to the lower frequency side with increasing ϕ_2. Similar behaviors have been reported for the dynamic moduli of PB and PS binary blends.[11,12] The reason for the shift of the upper plateau is conceivable from a molecular viewpoint: The terminal relaxation time of the 1-chains in the blended state increases to some extent from that in the pure state, i.e., $T_{d1} > T_{d1}^\circ$. Shift of T_{d1} with composition has been noted as[12]

$$T_{d1} = T_{d1}^\circ\left[\frac{d}{1-\phi_c}(\phi_2 - \phi_c) + 1\right] \quad \text{for} \quad \phi_2 > \phi_c \quad (29)$$

$$T_{d1} = T_{d1}^\circ \quad \text{for} \quad \phi_2 < \phi_c \quad (30)$$

where d is a constant representing the increment of relaxation time from its pure component value to its isolated value in a matrix of the 2-chains. This means that the terminal relaxation process of the 1-chains approaches pure reptation more closely when some of its tube-forming chains are long enough to impose more completely fixed obstacles upon the 1-chain.

Another remarkable observation is that the inflection occurs at an intermediate frequency between two plateaus. Figure 8 shows the variations of the slope for the master curves of G' of B95/575 blends. In this figure the inflection frequencies (marked by arrows), defining a local tube reorganization in that scale of frequencies, increase with increasing ϕ_2.

There are shown in Figure 9 the ϕ_2-dependences of the inverse of inflection frequency, $1/\omega_p$, and the intermediate storage modulus of the blend, $(G')_p$, corresponding to that frequency. The results show a concentration dependence of $(G')_p \propto \phi_2^{1.95}$. In earlier studies for binary blends of PS with the long chains in the short chains, $M_2 \gg M_1$, it is observed that $(G')_p \propto \phi_2^{1+\alpha}$. As the blend ratio approaches unity, that is, the blend becomes the monodisperse, the $(G')_p$ becomes equal to the plateau storage modulus $(G')_N$, resulting from the participation of all the chains in the entanglement network. The compositional dependence of the second plateau modulus is well predicted in eq 10. Additionally, it is appropriate that the weighting factor f_{22} is represented by eq 18.

On the other hand, the inverse of inflection frequency, $1/\omega_p$, is proportional to $\phi_2^{-0.85}$. That is, the tube renewal time T_{21} ($\propto 1/\omega_p$) slightly decreases with increasing ϕ_2. It is found that T_{21} in eq 5 is proportional to $\phi_2^{-2}T_{d1}$ and $T_{d1} \propto \phi_2$ in eq 29. As ϕ_2 increases, the 2–2 entanglements increase and the fraction that underwent constraint release upon the 2-chain decreases. Thus the number of submolecules in the equivalent Rouse chain generating a new tube must be decreased with increasing ϕ_2. To date, however, several authors[10,11] have started the analyses by assuming that the reptation of the model chain and constraint release are uncorrelated. In this system, such a fixed-tube assumption is valid no longer.

In order to estimate T_{d2}, the Cole–Cole plot occasionally is utilized. For the binary mixture with the moderate blend ratio, the reciprocal of the peak frequency, $1/\omega_2$, in the low-frequency domain signifies the average relaxation time of the 2-chain. Figure 10 shows the variations of log $(1/\omega_2)$ with log ϕ_2 in the concentrated region. The triangles and the diamonds denote the data for B100/2700 at 160 °C and for B110/400 at 186 °C, respectively, by Montfort et al.[9,10] The circles represent the results for B95/575 blends studied here. The T_{d2} increases with increasing ϕ_2 as predicted in eq 11 because the interactions among the 2-chains increase more and more. As the blend ratio R

Table II
Characteristic Parameters for Binary Blends (from Literature)

sample	temp, °C	R	$(\phi_2)_{max}$	$(\eta_0)_1$	$(\eta_0)_2$	$(J_e^\circ)_1$	$(J_e^\circ)_2$	ref
				PS				
B125/267	129	2.14	0.30	3.27×10^8	4.53×10^9	0.79×10^{-6}	1.14×10^{-6}	6
B86.8/500	190	5.73	0.07	5.00×10^3	4.20×10^6	1.1×10^{-6}	2.00×10^{-6}	7
B97.2/411	192	4.23	0.09	1.00×10^4	1.25×10^6	1.10×10^{-6}	1.40×10^{-6}	8
B110/400	186	3.64	0.13	4.63×10^4	3.48×10^6	1.16×10^{-6}	1.32×10^{-6}	9
B100/2700	160	27	0.03	5.75×10^5	1.59×10^{10}	1.26×10^{-6}	3.16×10^{-6}	10
B120/970	140	8.1	0.06	1.99×10^7	3.55×10^{10}	0.83×10^{-6}	1.6×10^{-6}	25
				PB				
B40.7/435	25	10.7	0.05	1.35×10^4	4.79×10^7	1.78×10^{-7}	2.10×10^{-7}	12
B97.7/435	25	4.45	0.1	3.13×10^5	4.79×10^7	2.00×10^{-7}	2.10×10^{-7}	12
B174/435	25	2.5	0.15	2.95×10^6	4.79×10^7	1.82×10^{-7}	2.10×10^{-7}	12
B40.7/174	25	4.28	0.1	1.35×10^4	2.95×10^6	1.78×10^{-7}	1.82×10^{-7}	12

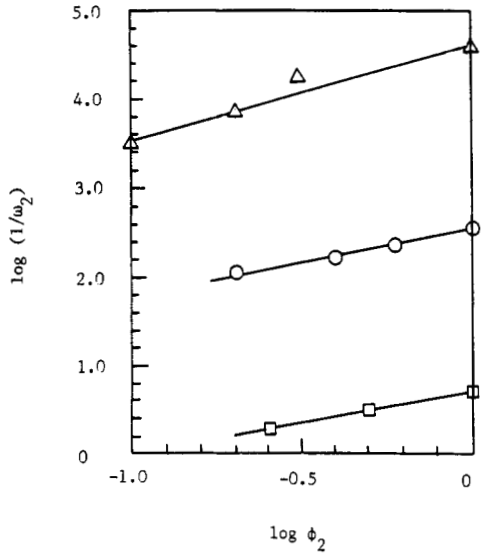

Figure 10. Variations of terminal relaxation times with ϕ_2. The symbols denote the data by Montfort et al. (□, △)[9,10] and that from this work (○).

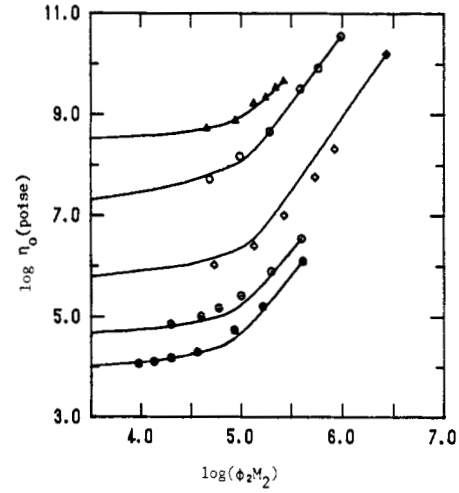

Figure 11. Variation of zero-shear viscosity η_0 with the extent of higher molecular component in binary blends. The lines are calculated from eq 32. The symbols denote the literature data by Prest (●),[8] Montfort et al. (⊙, ◇),[9,10] Zang et al. (○),[25] and Akovali (△).[6]

increases, the slope increases also. The variation of the slope with R is similar to that of eq 8, which means that T_{d2} increases with decreasing R ultimately to its pure component value T_{d2}° at $R \to 1$.

The dependences of T_{d1}, T_{21}, and T_{d2} on ϕ_2 and R are summarized as follows. T_{d1} is almost independent of R but increase slightly with ϕ_2. T_{21} decreases with increasing ϕ_2. T_{d2} increases with ϕ_2 and increases with increasing M_1.

3. Zero-Shear Viscosity. The zero-shear viscosity can be obtained by integration over the spectra:[1]

$$\eta_0 = \int_{-\infty}^{\infty} H(\tau)\, d \ln \tau \tag{31}$$

Employing eq 22 for the relaxation spectrum, we obtain the viscosity of the blend, $(\eta_0)_B$, as follows:

$$(\eta_0)_B = \phi_1(\eta_0)_1 + \phi_2(1 - \phi^\nu)\lambda_{21}(\eta_0)_2 + \phi_2\phi^{2\nu}(\eta_0)_2 \tag{32}$$

where $(\eta_0)_1$ and $(\eta_0)_2$ are the viscosities of their pure states, obtained from experimental data.

Usually, the viscosity η_0 is a function of M_w defined as

$$M_w = \phi_1 M_1 + \phi_2 M_2 \tag{33}$$

Especially, the η_0 is more sensitive to the extent of the higher molecular weight component. Figure 11 shows the dependence of η_0 on $\phi_2 M_2$ for the available literature data of the blends with high, intermediate, and low R's. The rheological characteristics of the samples borrowed from the literature are summarized in Table II. When R is large and M_1 small, the 2-chain behaves as a polymer in the solvent. That is, with increasing $\phi_2 M_2$, it is shown that the behavior moves from Rouse type, $\eta_0 \propto \phi_2 M_2$, to 3.4-power-law behavior, $\eta_0 \propto (\phi_2 M_2)^{3.4}$. It is conceivable that the constraint release upon the 2-chain dominates at low ϕ_2 but the reptation becomes more and more important with increasing ϕ_2. As the R decreases, however, the dependence of η_0 on $\phi_2 M_2$ deviates from those critical observations.

The lines in Figure 11 represent the $(\eta_0)_B$ estimated from eq 32. As shown in this figure, the present blending law is fitted well with all the data tested here. An inflection in the lines is observed at about $\phi_c M_2$ defined by eq 12. At high concentration, the $(\eta_0)_B$ is almostly dominated by the last term of eq 32. But the experimental data do not show the sharp inflection point and we cannot define the critical composition strictly. It may be caused by the residual polydispersity effect in each fraction with narrow MWD. It is shown in Figure 3 that the sharp transition is not observed in the data on the binary blends.

4. Recoverable Compliance. The compositional dependence of viscoelastic constants is very critical for testing the blending law. The recoverable compliance J_e° is very sensitive to the small amount of the high MW component. The J_e° is obtained from[1]

$$J_e^\circ(\eta_0)^2 = \int_0^\infty \tau H(\tau)\, d\tau \tag{34}$$

Thus, for the blend

$$(J_e^\circ)_B(\eta_0)_B^2 = \phi_1(\eta_0)_1^2(J_e^\circ)_1 + \lambda_{21}^2\phi_2(1 - \phi^\nu)(\eta_0)_2^2(J_e^\circ)_2 + \phi_2\phi^{3\nu}(\eta_0)_2^2(J_e^\circ)_2 \tag{35}$$

Figure 12 shows the relationship between J_e° and ϕ_2 for

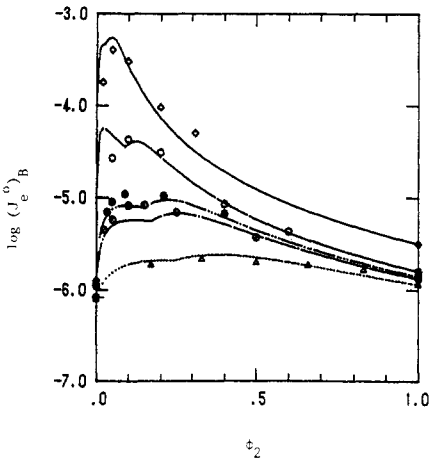

Figure 12. Compositional dependence of recoverable compliance J_e° in binary blends. The lines are calculated from eq 35 and the symbols are identified in Figure 11.

the blends as found by several authors. It is well-known that the compliance is a function of ϕ_2 and R and nearly independent of MW for each component. As R increases, the relation J_e° versus ϕ_2 approaches the behavior of the polymer in monomeric solvents. The current blending law for J_e° as well as η_0 is in good accord with the data over a wide range of ϕ_2 and R. At high concentration, eq 32 and 35 approach respectively

$$(\eta_0)_B = \phi_2^{1+2\nu}(\eta_0)_2 \quad (36)$$

$$(J_e^\circ)_B = \phi_2^{-(1+\nu)}(J_e^\circ)_2 \quad (37)$$

The above equations are well fitted with the data shown in Figures 11 and 12. As noticed in eq 37, it is predicted that the $(J_e^\circ)_B$ approaches $(J_e^\circ)_2$ by the relation $(J_e^\circ)_2/\phi_2$ at low R and the power law $(J_e^\circ)_2/\phi_2^2$ at high R. The ϕ_2-dependence of compliance at high ϕ_2 is well confirmed from the data over a wide range of R tested in Figure 12.

Observing the several data for J_e° of the binary mixtures, it has a maximum value at $\phi_2 = (\phi_2)_{max}$, which decreases with increasing R. The $(\phi_2)_{max}$ might be deeply related to the critical concentration ϕ_c due to the onset of entanglement between 2-chains. Figure 13 shows the ϕ_c by eq 12 and the $(\phi_2)_{max}$ in Table II for the data on PS[6-10] and PB[12] mixtures where both components are entangled. Both values shift to smaller ones with increasing R as expected. This figure gives satisfactory evidence that the onset of entanglement between long chains is represented by eq 12.

Conclusion

In order to account the viscoelastic properties of binary blends of flexible linear polymers, we presented a tube-model blending law including not only intramolecular chain dynamics, i.e., the contour length fluctuation, but also intermolecular relaxation mechanisms such as the reptation and the constraint release due to reptation of surrounding short chains upon the long chain. We have considered the constraint release as a local tube renewal between two entanglement points with 2–2 slip-links and demonstrated its effects by using the binary blends with a moderate blend ratio R. As expected, the tube renewal time T_{21} decreases with increasing ϕ_2 and the terminal relaxation time T_{d2} increases with ϕ_2.

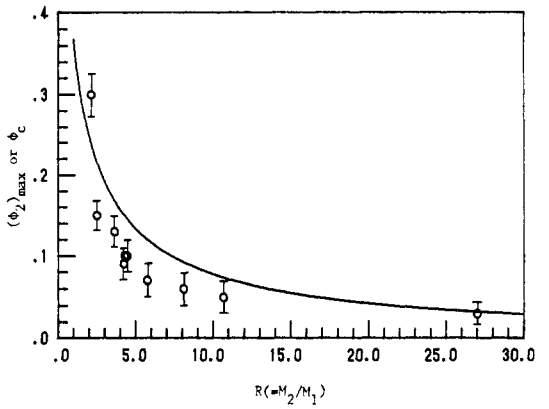

Figure 13. Variation of critical content of higher molecular component with the blend ratio R. The symbols denote the literature data summarized in Table II. The curve is calculated from eq 12.

The blending law here was compared with some other mixing laws proposed on the basis of the tube model so as to test the frequency dependence. The present blending law was compared also with various reported data on η_0 and J_e° of polystyrene over a wide range of R. Our proposal describes well the compositional dependence as well as the frequency dependence of rheological properties.

The onset of entanglement between different long chains is well represented by the blend ratio without regard to their constituent molecular weights.

Registry No. Polystyrene, 9003-53-6.

References and Notes

(1) Ferry, J. D. *Viscoelastic Properties of Polymers*, 3rd ed.; Wiley: New York, 1980.
(2) Graessley, W. W. *Adv. Polym. Sci.* **1974**, *16*, 1.
(3) Doi, M.; Kuzuu, N. Y. *J. Polym. Sci., Polym. Lett. Ed.* **1980**, *18*, 775.
(4) Pearson, D. S.; Helfand, E. *Macromolecules* **1984**, *17*, 888.
(5) Struglinski, M. J. Doctorial Thesis, Northwestern University, 1984.
(6) Akovali, A. *J. Polym. Sci., Polym. Phys. Ed.* **1967**, *5*, 875.
(7) Mills, N. J.; Nelvin, A. J. *J. Polym. Sci., Polym. Phys. Ed.* **1971**, *9*, 267.
(8) Prest, W. M.; Porter, R. S. *Polym. J. (Tokyo)* **1973**, *10*, 445.
(9) Montfort, J. P. *Polymer* **1976**, *17*, 1054.
(10) Montfort, J. P.; Marin, G.; Monge, D. *Macromolecules* **1984**, *17*, 1551; *Macromolecules* **1986**, *19*, 1979.
(11) Watanabe, H.; Kotaka, T. *Macromolecules* **1984**, *17*, 2316; Watanabe, H.; Sakamoto, T.; Kotaka, T. *Macromolecules* **1985**, *18*, 1008.
(12) Struglinski, M. J.; Graessley, W. W. *Macromolecules* **1985**, *18*, 2630, 2643.
(13) Daoud, M.; de Gennes, P. G. *J. Polym. Sci., Polym. Phys. Ed.* **1979**, *17*, 1971.
(14) Ninomiya, K.; Ferry, J. D. *J. Colloid Sci.* **1963**, *18*, 421.
(15) Prest, W. M. *Polym. J. (Tokyo)* **1971**, *4*, 163.
(16) Kurata, M. *Macromolecules* **1984**, *17*, 895.
(17) Doi, M.; Edwards, S. F. *J. Chem. Soc., Faraday Trans. 2* **1978**, *74*, 1789, 1802, 1818; **1979**, *75*, 38.
(18) Kim, H. Y.; Chung, I. J. *J. Polym. Sci., Polym. Phys. Ed.* **1987**, *25*, 2039.
(19) de Gennes, P. G. *J. Chem. Phys.* **1971**, *55*, 572.
(20) Doi, M. *J. Polym. Sci., Polym. Lett. Ed.* **1981**, *19*, 265; *J. Polym. Sci., Polym. Phys. Ed.* **1983**, *21*, 667.
(21) Lin, Y. H. *Macromolecules* **1984**, *17*, 2846.
(22) Klein, J. *Macromolecules* **1978**, *11*, 852.
(23) Graessley, W. W. *Adv. Polym. Sci.* **1982**, *47*, 67.
(24) Osaki, K.; Nishizawa, K.; Kurata, M. *Macromolecules* **1982**, *15*, 1068.
(25) Zang, Y. H.; Muller, R.; Froelich, D. *Polymer* **1987**, *28*, 1577.